

# Electron Spin Resonance Studies of Silver Atom Solvation in Ethanol-Water Mixtures. Evidence for Preferential Solvation

Anson S. W. Li and Larry Kevan\*

Department of Chemistry, Wayne State University, Detroit, Michigan 48202 (Received: April 30, 1980)

Frozen solutions of silver perchlorate exposed to  $^{60}\text{Co}$   $\gamma$  irradiation at 4 K form silver atoms by reaction of radiation-produced electrons with the silver ion. At 4 K the silver atoms are initially produced in a nonequilibrium or presolvated state, and upon brief warming to 77 K the first solvation shell geometry changes to produce an equilibrium or solvated silver atom. The presolvated and solvated silver atoms in water and ethanol matrices are characterized by different isotropic hyperfine couplings and line widths measured by electron spin resonance. We have investigated silver atoms in water-ethanol mixtures to search for preferential solvation effects. From 0 to 13 mol % ethanol the presolvated silver atom formed at 4 K exhibits parameters characteristic of a water environment. At 13 mol % the parameters *suddenly* change to those characteristic of an ethanol environment. This suggests that the original silver ion undergoes a drastic change in its first solvation shell at 13 mol % ethanol. This dramatic change appears to correlate with the minimum in the excess enthalpy of mixing of ethanol and water vs. ethanol mole percent. Further solvation changes occur on thermal annealing the silver atoms at 77 K.

## Introduction

Recent electron spin resonance (ESR) and electron spin-echo studies of silver atom solvation in water and in methanol have resulted in a geometrical picture of atom solvation at the molecular level.<sup>1-4</sup> Frozen solutions of silver salts exposed to  $\gamma$  irradiation form silver atoms by reaction of radiation-produced electrons with the silver ions. It was found that  $\text{Ag}^0$ , when first formed in ice at 4 K ( $\text{Ag}^0/\text{H}_2\text{O}$ ), is in a presolvated or nonequilibrium state which is characterized by an isotropic hyperfine splitting of 1763 MHz for  $^{109}\text{Ag}$ .<sup>3</sup> The geometry of this state corresponds to four water molecules arranged tetrahedrally about  $\text{Ag}^0$  with the negative end of each water dipole oriented toward  $\text{Ag}^0$ . Upon annealing at 77 K,  $\text{Ag}^0$  is converted to a near-equilibrium, solvated state characterized by a  $^{109}\text{Ag}$  splitting of 1461 MHz in which *one* of the four water molecules has reoriented to bring one H  $\approx 1$  Å closer to the  $\text{Ag}^0$ . The driving force for this site conversion probably involves hydrogen bonding.

A contrasting situation was found for  $\text{Ag}^0$  in methanol ( $\text{Ag}^0/\text{MeOH}$ ).<sup>4</sup> The first solvation shell geometry of  $\text{Ag}^0/\text{MeOH}$  formed at 4 K, deduced from electron spin-echo measurements, undergoes no detectable change upon brief annealing at 77 K. Consistent with this there is only a small decrease in the  $^{109}\text{Ag}$  isotropic hyperfine constant at 4 K and after brief annealing to 77 K.<sup>5</sup> The lack of a significant geometrical change on annealing has been interpreted as due to the less acidic character of the hydroxyl proton of methanol compared to that of water which leads to a weaker hydrogen bonding interaction between  $\text{Ag}^0$  and methanol.

Here we investigate silver atom solvation in ethanol and explore the difference between solvation in alcohol and water by examining the relationship between hyperfine splittings and alcohol concentration in ethanol-water mixtures.

## Experimental Section

Solutions of 0.5 M  $\text{AgClO}_4$  + 0.2 M NaF in various ethanol-water mixtures were prepared. The NaF acts as a hole trap and greatly enhances the  $\text{Ag}^0$  yield.<sup>6</sup> The samples contained  $\sim 0.15$  mL of solution in 4.2-mm o.d. Spectrosil tubes. Samples were irradiated in liquid helium in an ESR Dewar with a Siemens X-ray tube (Model AGW61) connected to a Kristalloflex-2 power supply. All

irradiations were carried out at 60 kV and 50 mA; doses were typically 0.4 Mrd at a dose rate of 0.8 Mrd  $\text{h}^{-1}$ . Spectra were obtained with a Varian E-102 ESR spectrometer. Annealing at 77 K was done by removing the sample tubes from liquid helium, plunging them into liquid nitrogen for a specified time, and reinserting them into liquid helium. The frequency was measured directly with a microwave frequency counter. The calibration of the field sweep and the field was checked against the hyperfine splitting and  $g$  factor of hydrogen atoms trapped in irradiated Spectrosil tubes<sup>7</sup> in which the samples were measured. The ESR parameters were derived from the Breit-Rabi equation.<sup>8</sup>

## Results

Naturally occurring silver consists of 48%  $^{109}\text{Ag}$  and 52%  $^{107}\text{Ag}$ , each of which has a nuclear spin  $I = 1/2$ . One hyperfine doublet arises from each isotope resulting in a four-line spectrum. The ratio of the nuclear moments [ $g(109)/g(107) \approx 1.15$ ] of the two silver isotopes is large enough to permit resolution of all four lines with the bigger splitting assigned to  $^{109}\text{Ag}$ . The spectra were taken with 6-kHz field modulation. The center portions of the spectra have been deleted in the figures in order to emphasize the portions of the silver spectra of interest.

The spectra of  $\text{Ag}^0/\text{H}_2\text{O}$  and  $\text{Ag}^0/\text{EtOH}$  after irradiation and observation at 4 K are shown in Figures 1 and 2. H indicates trapped hydrogen atoms in the sample tube. The ESR first derivative peak-to-peak line widths at high field are  $13 \pm 0.5$  MHz in  $\text{H}_2\text{O}$  and  $49 \pm 1$  MHz in EtOH. The isotropic hyperfine splittings of  $^{109}\text{Ag}$  are  $1756 \pm 2$  MHz in  $\text{H}_2\text{O}$  and  $1793 \pm 2$  MHz in EtOH. These are the presolvated states and are denoted as site WI in  $\text{H}_2\text{O}$  and site EI in EtOH. The  $g$  factors are 1.9993 in  $\text{H}_2\text{O}$  and 1.9999 in EtOH.

Samples in the range of 0-13 mol % ethanol after irradiation and observation at 4 K show the same spectra as that obtained in pure water. The sample of 13 mol % is shown in Figure 3 as an example for samples in this concentration range. From 14 to 100 mol % ethanol, the general shape of the spectra, both in line width and hyperfine splitting, resembles that obtained in pure ethanol. Figure 4 shows the 14 mol % sample as an example in this concentration range. From 13 to 14 mol % the spectral shape suddenly changes from a waterlike to an ethanol like

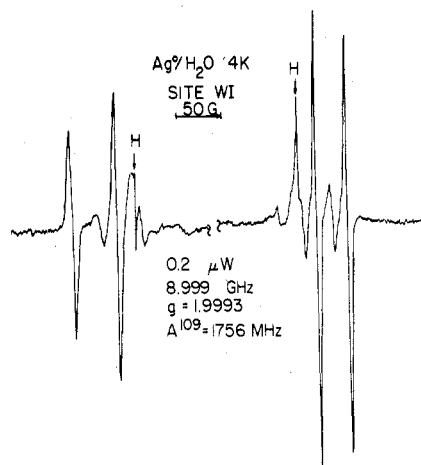


Figure 1. ESR spectrum at 4 K of  $\text{Ag}^0$  in X-irradiated (0.4 Mrd) 0.5 M  $\text{AgClO}_4$  plus 0.2 M NaF aqueous solution. The microwave power is  $0.2 \mu\text{W}$  and the frequency is 8.999 GHz.

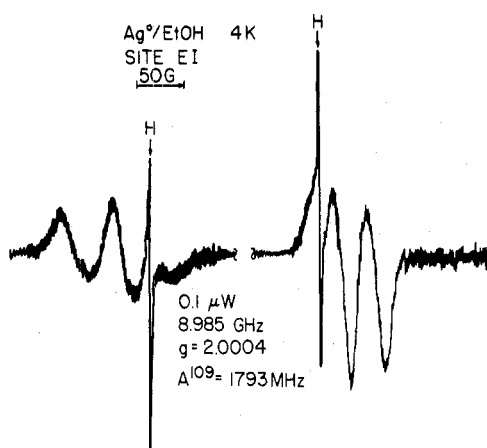


Figure 2. ESR spectrum at 4 K of  $\text{Ag}^0$  in X-irradiated (0.4 Mrd) 0.5 M  $\text{AgClO}_4$  plus 0.2 M NaF ethanol solution. The microwave power is  $0.1 \mu\text{W}$  and the frequency is 8.985 GHz.

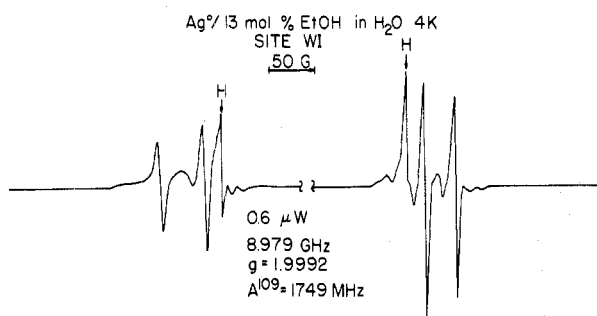


Figure 3. ESR spectrum at 4 K of  $\text{Ag}^0$  in X-irradiated (0.4 Mrd) 0.5 M  $\text{AgClO}_4$  plus 0.2 M NaF in 13 mol % ethanol in water solution. The microwave power is  $0.6 \mu\text{W}$  and the frequency is 8.979 GHz.

spectrum. Figure 5 shows the change of the hyperfine splitting with ethanol concentration.

Brief (15 s) warming at 77 K followed by observation at 4 K causes rearrangement of the silver atom environment to generate a new site characterized by changes of the silver hyperfine splitting,  $g$  factor, and spectral line width. Figures 6 and 7 show the spectra for annealed  $\text{Ag}^0/\text{H}_2\text{O}$  and  $\text{Ag}^0/\text{EtOH}$ , respectively. The line widths at high field are  $33 \pm 1$  MHz in  $\text{H}_2\text{O}$  and  $32 \pm 1$  MHz in EtOH. The isotropic hyperfine splittings of  $^{109}\text{Ag}$  are  $1456 \pm 1$  MHz in  $\text{H}_2\text{O}$  and  $1740 \pm 1$  MHz in EtOH. These are near equilibrium solvated states and are denoted as site WII in  $\text{H}_2\text{O}$  and site EIIA in EtOH. Actually site EI separates into sites EIIA and EIIB upon annealing. This

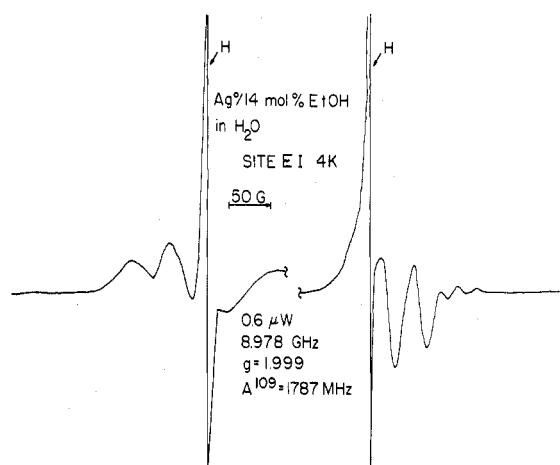


Figure 4. ESR spectrum at 4 K of  $\text{Ag}^0$  in X-irradiated (0.4 Mrd) 0.5 M  $\text{AgClO}_4$  plus 0.2 M NaF in 14 mol % ethanol in water solution. The microwave power is  $0.6 \mu\text{W}$  and the frequency is 8.978 GHz.

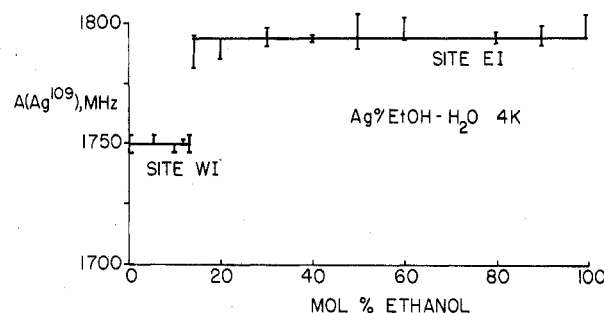


Figure 5. The change in isotropic hyperfine splitting of presolvated  $\text{Ag}^0$  directly produced at 4 K with increasing ethanol concentration.

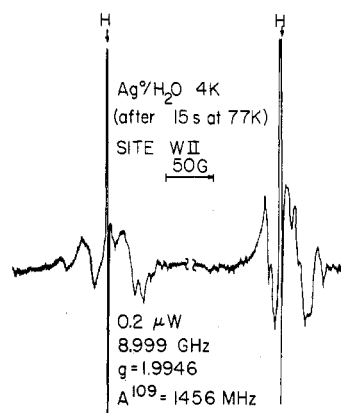


Figure 6. The same sample as in Figure 1,  $\text{Ag}^0/\text{H}_2\text{O}$ , after 15-s annealing at 77 K.

is shown by arrows in Figure 7. The intensity ratio of site EIIA to EIIB increases with an increase in ethanol concentration. It is also observed that further annealing at 77 K increases the splitting of  $\text{Ag}^0/\text{H}_2\text{O}$  which finally becomes  $1522 \pm 2$  MHz. There is no detectable change in the splitting of  $\text{Ag}^0/\text{EtOH}$  upon further annealing at 77 K. Figures 8 and 9 show annealed samples of 13 and 14 mol % ethanol, respectively. The site W as shown in Figure 8 is a  $\text{Ag}^0/\text{H}_2\text{O}$  site which is also observed in Figure 1 before annealing. This site is observed at 4 K and does not change upon 77 K annealing. There is another site, site 2020, as indicated by arrows in Figure 8, which shows up only in annealed ethanol-water mixtures but not in either pure component. This site is observed in the range of 5–60 mol % ethanol. The high-field line width is  $10 \pm 0.5$  MHz, and the  $^{109}\text{Ag}$  isotropic hyperfine splitting is  $2020 \pm 1$  MHz. The splitting of this site 2020 is independent

TABLE I: Hyperfine Splittings,  $g$  Factors, and High-Field Line Widths in Ethanol-Water Mixtures for  $^{109}\text{Ag}$  Atoms Produced at 4 K and After Annealing to 77 K<sup>b</sup>

EtOH, mol %	4 K				4 K $\rightarrow$ 77 K $\rightarrow$ 4 K			
	site	$g^a$	$A$ , MHz	$\Delta\nu_{pp}$ , MHz	site	$g^a$	$A$ , MHz	$\Delta\nu_{pp}$ , MHz
0	WI	1.9993 $\pm$ 2	1756 $\pm$ 1	14	WII	1.9947 $\pm$ 2	1457 $\pm$ 2	33
5	WI	1.9990 $\pm$ 2	1751 $\pm$ 2	14	WII	1.9950 $\pm$ 3	1461 $\pm$ 6	33
10	WI	1.9992 $\pm$ 2	1747 $\pm$ 1	14	WII	1.9952 $\pm$ 5	1460 $\pm$ 5	33
12	WI	1.9990 $\pm$ 2	1750 $\pm$ 1	14	WII	1.9964 $\pm$ 5	1470 $\pm$ 2	33
13	WI	1.9992 $\pm$ 4	1749 $\pm$ 4	14	WII	1.9968 $\pm$ 5	1466 $\pm$ 5	33
14	EI	1.9985 $\pm$ 13	1787 $\pm$ 7	48	2020	2.0007 $\pm$ 3	2022 $\pm$ 2	13
20	EI	1.9982 $\pm$ 6	1789 $\pm$ 4	48	2020	2.0007 $\pm$ 1	2019 $\pm$ 2	13
30	EI	1.9982 $\pm$ 4	1794 $\pm$ 4	48	2020	2.0008 $\pm$ 1	2018 $\pm$ 4	13
40	EI	1.9988 $\pm$ 4	1794 $\pm$ 1	48	2020	2.0004 $\pm$ 1	2022 $\pm$ 2	13
50	EI	1.9995 $\pm$ 10	1796 $\pm$ 7	48	2020	2.0005 $\pm$ 1	2022 $\pm$ 4	13
60	EI	1.9985 $\pm$ 10	1797 $\pm$ 4	48	2020	2.0008 $\pm$ 1	2019 $\pm$ 3	13
80	EI	1.9988 $\pm$ 1	1793 $\pm$ 2	48	EII	1.9984 $\pm$ 4	1747 $\pm$ 8	32
90	EI	1.9989 $\pm$ 5	1794 $\pm$ 4	48	EII	1.9986 $\pm$ 2	1738 $\pm$ 2	32
100	EI	2.0004 $\pm$ 7	1797 $\pm$ 5	48	EII	1.9994 $\pm$ 7	1732 $\pm$ 3	32

<sup>a</sup> The uncertainties refer to the last one or two digits in the  $g$  factor. <sup>b</sup> All measurements were made at 4 K. The uncertainties given are average deviations.

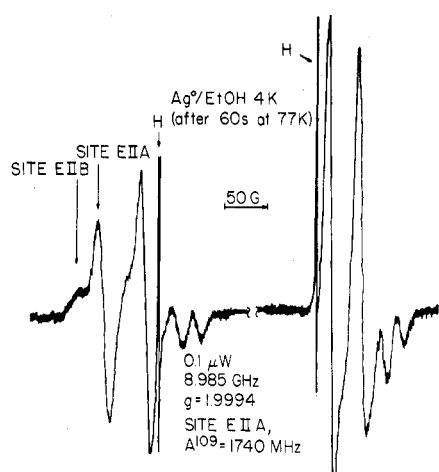


Figure 7. The same sample as in Figure 2,  $\text{Ag}^0/\text{EtOH}$ , after 60-s annealing at 77 K.

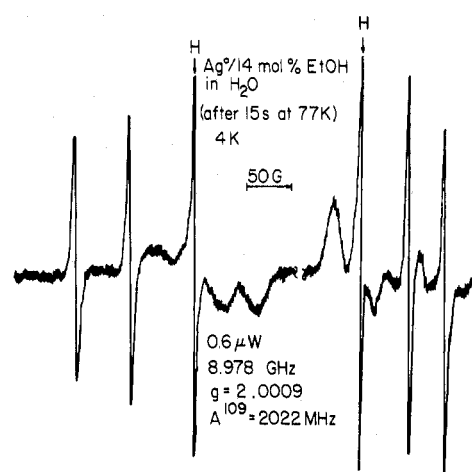


Figure 9. The same sample as in Figure 4,  $\text{Ag}^0$  in 14 mol % ethanol, after 15-s annealing at 77 K.

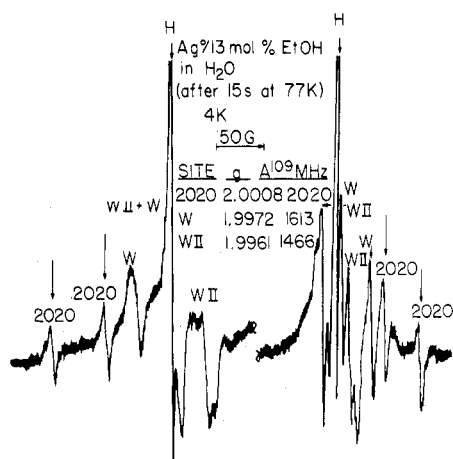


Figure 8. The same sample as in Figure 3,  $\text{Ag}^0$  in 13 mol % ethanol, after 15-s annealing at 77 K.

of both ethanol concentration and time after irradiation. The intensity of this site decreases with increasing ethanol concentration and increases, though with different rates at different ethanol concentrations, with time after irradiation. It becomes the only observable  $\text{Ag}^0$  peak for samples in the range of 13–50 mol % ethanol. In the range of 5–13 mol % ethanol, both site WII and site 2020 are observed. In the range of 50–60 mol % ethanol, site 2020 and site EII are both observed in such a way that site 2020 decreases and site EII increases with an increase in ethanol

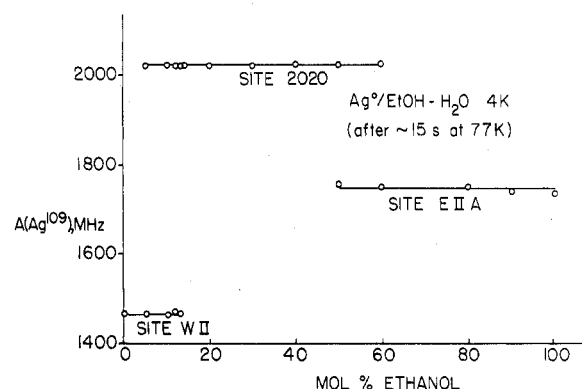
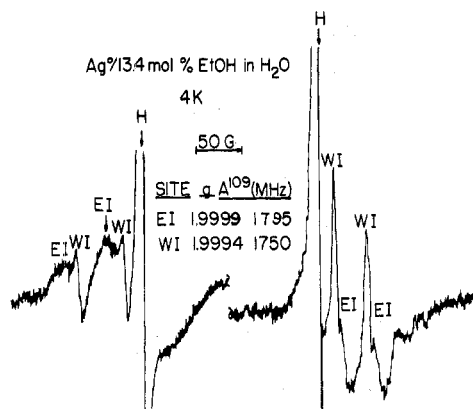


Figure 10. The isotropic hyperfine splitting of various  $\text{Ag}^0$  sites vs. ethanol concentration after 77 K annealing.

concentration. Site 2020 becomes undetectable for samples of ethanol concentration larger than 60 mol %. A summary of these results is depicted in Figure 10.

Irradiation of silver salts in ethanol at 77 K also generates ESR lines assigned to  $\text{Ag}_2^+$  formed by reaction of  $\text{Ag}^0$  with  $\text{Ag}^+$ .<sup>9</sup> The peaks of  $\text{Ag}_2^+$  are not observed after irradiation at 4 K in pure ethanol, but they do show up after 77 K annealing. On storing at 77 K in the dark, eventually all  $\text{Ag}^0$  converts to  $\text{Ag}_2^+$  for samples in the range of 80–100 mol % ethanol.

The  $g$  factors calculated for  $^{109}\text{Ag}$  are shown in Table I for the entire range of ethanol-water mixtures. For the atoms initially produced at 4 K there is no significant



**Figure 11.** ESR spectrum at 4 K of  $\text{Ag}^0$  in X-irradiated (0.4 Mrd) 0.5 M  $\text{AgClO}_4$  plus 0.2 M NaF in 13.4 mol % ethanol in water solution. The microwave power is 0.8  $\mu\text{W}$  and the frequency is 8.992 GHz.

change with respect to ethanol concentration. There is a change, however, in the  $g$  factor for samples of 0–13 mol % ethanol after 77 K annealing. This change from 1.999 to 1.996 is in good agreement with previous results.<sup>3</sup>

### Discussion

First, we discuss the effect of bulk solvent composition on the local environment of silver atoms generated by radiolysis at 4 K. This is considered to be a nonequilibrium environment for the silver atom since it is suddenly produced from the ion by electron addition at 4 K where the thermal energy is insufficient to induce an equilibrium rearrangement of the local environment from that for a silver ion to that for a silver atom. The local environment is characterized by the isotropic hyperfine interaction, the  $g$  factor, and the line width. Table I shows that these characteristics are distinctly different for silver atoms formed at 4 K in ice and in ethanol. In mixed solvents one normally expects a progressive gradual change in the solvation shell environment of an ion or atom as the bulk solvent composition is changed. However, from the results in Table I it is clear that this is not the case for silver atoms generated in water–ethanol mixtures. Instead, between 13 and 14 mol % ethanol there is a *sudden* change in the isotropic hyperfine coupling to the silver nucleus and in the line width.

To examine this point more critically, we have shown the spectrum of silver atoms in 13.4 mol % ethanol generated at 4 K in Figure 11. The spectrum shows site WI superimposed on top of site EI. This implies that no mixed water–ethanol solvation shell for the silver atoms exists. In the transition concentration range it appears that two distinctly different solvation shell environments for the silver atoms exist rather than a gradual change from one environment to the other involving a mixed solvation shell.

After the samples are annealed at 77 K, Table I shows that distinct changes occur in the isotropic hyperfine constant to the silver nucleus and in the line width both for silver atoms in the water environment from 0 to 13 mol % ethanol and for silver atoms in the ethanol environment from 14 to 100% ethanol. However, the sudden change in the apparent local environment of the silver atoms between 13 and 14 mol % ethanol is retained even after annealing at 77 K.

Up to this point we have assumed that the sudden change in the magnetic parameters of the trapped silver atoms between 13 and 14 mol % ethanol has indicated a change from a water environment to an ethanol environment. However, we point out that it is also possible that this sudden change is associated with a change in phase from a predominantly polycrystalline environment to a

predominantly glassy environment. Frozen aqueous solutions of silver salts form an apparently crystalline solid as indicated by its opaqueness, whereas ethanol frozen solutions form glasses as indicated by their transparency. We do observe that in the range near 13–14 mol % there is a change in the apparent glassiness or polycrystalline character of the frozen mixed solvent. However, visually this change is not as sudden as the change that the magnetic resonance parameters indicate. One argument against the assignment of the change in the magnetic resonance parameters to an apparent phase transition between a polycrystalline to a glassy environment is that annealing to 77 K does not affect the composition at which this apparent change in the magnetic resonance parameters occurs. Normally, annealing at a higher temperature causes a glass to partially crystallize, and for a mixed solvent one expects that 77 K annealing would shift the composition at which an apparent sudden transition from a polycrystalline to a glassy environment occurred. In fact, the transition should be shifted to lower mole fractions of ethanol, but this is not the case as seen in Table I.

We find it difficult to conceive of a physical reason for the suddenness of the change from an apparent water environment to an apparent ethanol environment between 13 and 14 mol % ethanol. However, we note that the change at this composition corresponds to the minimum in the excess enthalpy of mixing for ethanol–water liquid mixtures.<sup>10,11</sup> This thermodynamic change has been interpreted as due to preferential hydrogen bonding between water and ethanol to form well-defined complexes in the liquid state at room temperature. It is probable that such complexes would be frozen in on rapid freezing to 4 K. These could constitute different trapping environments for the silver atom and could relate to the abrupt change in the magnetic resonance parameters that is observed in this mole fraction range. The composition dependence of sound absorption coefficients in ethanol–water mixtures<sup>10,11</sup> has also been interpreted as due to ethanol–water complex formation in the same composition range as suggested by the thermodynamic data. It should be pointed out that the interpretation of the thermodynamic and sound absorption data in terms of ethanol–water complexes is speculative. Both our data and the thermodynamic and sound absorption data do indicate some sort of drastic environmental change between 13 and 14 mol % ethanol in ethanol–water mixtures. The exact molecular nature of this structural change is not clear. It is conceivable that preferential hydrogen bonding between water and ethanol molecules could control the balance between preferential water solvation of silver atoms and preferential ethanol solvation of silver atoms.

It is also of considerable interest that hydrogen atoms produced by radiolysis are trapped at 77 K in ethanol–water mixtures and have a maximum yield at 13.5 mol % ethanol.<sup>12</sup> This was interpreted as a local environmental change in the mixture that led to a structure that was particularly favorable for the trapping of hydrogen atoms at 77 K. This is all the more remarkable since hydrogen atoms are not trapped either in pure ethanol or in pure water at 77 K. It seems reasonable that the same specific structural local environments could give rise to the sudden change in magnetic resonance parameters found for trapped silver atoms in ethanol–water mixtures.

Annealing at 77 K of the silver atom initially trapped in ice at 4 K leads to a significant change in magnetic resonance parameters which is shown in Table I. This has been interpreted as due to a rearrangement of one of four water molecules per solvation shell to create a relatively

strong hydrogen bond between the silver atom and that water molecule.<sup>1-3</sup> This has been totally supported by detailed structural studies by electron spin-echo spectrometry.<sup>2,3</sup> In pure ethanol the effect of 77 K annealing also causes a change in the isotropic hyperfine constant of the silver nucleus and in the line width as shown in Table I. However, the decrease in the isotropic coupling constant is only ~60 MHz in the case of ethanol, whereas it is ~300 MHz in the case of water. This indicates that there is indeed some structural change in the silver atom environment in the ethanol matrix after 77 K annealing. This can be interpreted as a change toward an equilibrium structure which we may term solvation. However, the much smaller change in the magnetic resonance parameters in the case of the silver atom in ethanol compared to water indicates that no drastic rearrangement of the solvation structure occurs in ethanol whereas quite a drastic rearrangement occurs in the case of a water matrix. This is consistent with earlier studies by electron spin-echo spectrometry to probe the local environment of silver atoms trapped in methanol.<sup>4</sup> The spin-echo study could not detect a change in the average distance between the silver nucleus and the nearest protons in the first solvation shell in the case of methanol,<sup>4</sup> whereas such a change is easily observed in the case of water.<sup>1</sup> The case of silver atoms in ethanol seems similar to that for silver atoms in methanol in that no drastic rearrangement occurs, although some local environmental change is detected by the change in the isotropic hyperfine constant of the silver. Since the silver isotropic hyperfine constant is so large, even a very minor environmental change corresponding to less than 0.1 Å change in distance between the silver nucleus and the first solvation shell proton nuclei could cause an observable change in the silver isotropic hyperfine coupling. This relatively small change is of course consistent with the weaker hydrogen-bonding ability expected for a silver atom in alcohol compared to water.

Between 5 and 60 mol % ethanol annealing at 77 K produces a new silver site with a remarkably large silver isotropic hyperfine constant of ~2020 MHz. This splitting is even larger than that of a free silver atom for <sup>109</sup>Ag, which is 1977 MHz.<sup>13</sup> The 2020-MHz splitting can be rationalized by a contraction of the silver wave function onto the silver nucleus due to Pauli exclusion repulsion between the 5s silver electron and the electrons on the first solvation shell molecules. It is interesting that this 2020 site shows up only after 77 K annealing in a certain range of ethanol-water mixtures but not in either pure component. This perhaps implies that the 2020 site is associated with some sort of an interstitial site for the silver atom in the mixtures which does not occur in either of the pure components.

Our results after 77 K annealing may be compared with previous results reported for silver atom production in ethanol-water mixtures irradiated only at 77 K.<sup>14</sup> However, there are some differences between our results and these earlier experiments. It was earlier reported that 77 K irradiation produces silver atoms which convert only to site 2020 after annealing in the range of 130-180 K for 13-65 mol % ethanol. However, we observed that this site is produced by annealing at 77 K without going to higher temperatures. Also we have carried out experiments by

irradiating directly at 77 K in which we observe the 2020 site without any thermal annealing above this temperature. In earlier work at 77 K a sudden change in hyperfine parameters near 13-14 mol % ethanol was observed, although no molecular interpretation of this effect was offered. A silver atom site in the range of 13-65 mol % ethanol with a <sup>109</sup>Ag splitting of 1346 MHz was also reported. However, we do not observe this site for either irradiation at 4 or 77 K.

Finally, we comment on the formation of Ag<sub>2</sub><sup>+</sup>. In previous work in ice and in alcohol matrices, it has been postulated that some motion is necessary for the formation of Ag<sub>2</sub><sup>+</sup>.<sup>15,16</sup> For example, in ice matrices Ag<sub>2</sub><sup>+</sup> is not formed by radiolytic generation of silver atoms at 77 K but is formed after annealing to 160 K. Presumably this allows some of the silver atoms to react with nearby or not so nearby silver ions to form the complex ions. However, in alcohol matrices, in particular methanol and ethanol, Ag<sub>2</sub><sup>+</sup> is formed directly by radiolysis at 77 K. This has been postulated to be due to a greater degree of mobility in the alcohol matrix than in the ice matrix at 77 K.<sup>16</sup> This has been verified in the present experiment in that no Ag<sub>2</sub><sup>+</sup> is formed in pure ethanol matrices at 4 K whereas it is generated after annealing to 77 K. However, of significant interest is that Ag<sub>2</sub><sup>+</sup> is formed in a very small amount after 4 K radiation in ethanol-water mixtures. This indicates that there is more mobility for the silver atoms generated in the ethanol-water mixtures than in either pure ethanol or pure water at 4 K. This inferred greater degree of mobility in the ethanol-water mixtures is physically reasonable if complexes are formed between the ethanol and water molecules which serve to somewhat disrupt the structure in the mixture. This is at least qualitatively consistent with the picture which has been deduced above for the sudden change from an apparent water environment below 13 mol % ethanol to an apparent ethanol environment above 14 mol % ethanol in the ethanol-water mixtures.

*Acknowledgment.* This work was partially supported by the U. S. Department of Energy under Contract No. EY-S-02-2086. A. Li acknowledges a Graduate Fellowship from Wayne State University.

## References and Notes

- (1) L. Kevan, H. Hase, and K. Kawabata, *J. Chem. Phys.*, **66**, 3834 (1977).
- (2) P. A. Narayana, D. Becker, and L. Kevan, *J. Chem. Phys.*, **68**, 652 (1978).
- (3) L. Kevan, *J. Chem. Phys.*, **69**, 3444 (1978).
- (4) T. Ichikawa, L. Kevan, and P. A. Narayana, *J. Phys. Chem.*, **83**, 3378 (1979).
- (5) A. Li and L. Kevan, unpublished results.
- (6) B. L. Bales and L. Kevan, *J. Phys. Chem.*, **74**, 1098 (1970).
- (7) S. Ogawa and R. W. Fessenden, *J. Chem. Phys.*, **41**, 1516 (1964).
- (8) G. Breit and I. Rabi, *Phys. Rev.*, **38**, 2082 (1931).
- (9) L. Shields, *J. Chem. Phys.*, **44**, 1685 (1966).
- (10) F. Franks in "Physico-Chemical Processes in Mixed Aqueous Solvents", F. Franks, Ed., American Elsevier, New York, 1967, pp 50-70; see especially pp 54-6.
- (11) F. Franks and D. J. G. Ives, *Q. Rev., Chem. Soc.*, **20**, 1 (1966).
- (12) H. Hase and L. Kevan, *J. Phys. Chem.*, **74**, 3355 (1970).
- (13) L. Shields, *J. Chem. Phys.*, **55**, 1327 (1971).
- (14) R. A. Zhitnikov and D. P. Peregud, *Fiz. Tverd. Tela*, **12**, 1993 (1970); *Sov. Phys.—Solid State (Engl. Transl.)*, **12**, 1583 (1971).
- (15) B. L. Bales and L. Kevan, *J. Chem. Phys.*, **55**, 1327 (1971).
- (16) J. Michalik and L. Kevan, *J. Magn. Reson.*, **31**, 259 (1978).